



Decreased gas-diffusion electrode porosity due to increased electrocatalyst loading leads to diffusional limitations in cathodic H₂O₂ electrosynthesis

Emily Murawski^a, Negin Kananizadeh^a, Spencer Lindsay^a, Apparao M. Rao^b, Sudeep C. Popat^{a,*}

^a Department of Environmental Engineering and Earth Sciences, Clemson University, 342 Computer Ct, Anderson, SC, 29625, United States

^b Department of Physics and Astronomy, Clemson Nanomaterials Institute, Clemson University, 81 Technology Dr., Anderson, SC, 29625, United States

HIGHLIGHTS

- Increased electrocatalyst loading on GDE lowers efficiency of H₂O₂ electrosynthesis.
- Increased electrocatalyst loading decreases GDE porosity.
- Decreased GDE porosity likely affects H₂O₂ mass transport.
- Electrolyte pH plays a significant role in H₂O₂ production.

ARTICLE INFO

Keywords:

Peroxide
Electrosynthesis
Gas-diffusion cathode
Electrocatalyst loading
X-ray CT

ABSTRACT

The effect of carbon black electrocatalyst loading on the efficiency of cathodic hydrogen peroxide (H₂O₂) electrosynthesis in neutral buffered catholytes using gas-diffusion electrodes (GDEs) was evaluated. Increased carbon black loadings on carbon cloth-based GDEs (from 0.5 to 1.5 mg/cm² to 3.3 mg/cm²) reduced the cathodic coulombic efficiency significantly although no significant advantage in terms of electrochemical performance was noted for the highest loading studied in linear sweep voltammograms. Decreasing cathodic coulombic efficiency during a given batch H₂O₂ electrosynthesis experiment was a result of increasing catholyte pH, which occurred irrespective of the carbon black loading, and could be alleviated using a higher buffer concentration. Scanning electron microscopy (SEM) and X-ray computed tomography (CT) reconstructions of the GDEs with the different carbon black loadings showed that increased loading leads to lower GDE porosity, which likely causes mass transport limitations, that result in consumption of H₂O₂ *in-situ* in the electrocatalyst layer, either due to electrochemical reduction or decomposition in high pH conditions. Future studies should focus on engineering GDE structures that allow enhanced mass transport rates for H₂O₂ out of the GDE, thus also achieving high coulombic efficiencies.

1. Introduction

Hydrogen peroxide (H₂O₂) is an important industrial chemical that is currently produced primarily through the anthraquinone process, which uses large amounts of energy and expensive catalysts, and produces toxic intermediates [1]. Electrochemical synthesis of H₂O₂ via the cathodic reduction of oxygen (O₂), as shown in equation (1), is increasingly being researched to provide an alternative to the anthraquinone process that is safe, efficient and energy-positive or -neutral especially if linked to a chemical or biological fuel cell [2–6]. The

electrosynthesis of H₂O₂ especially in microbial fuel cells (MFCs) has been of keen interest recently as in this route, the chemical energy present in waste organics is converted to electrical current to power the production of H₂O₂ for on-site use [7–11]. Such MFCs could potentially be incorporated in H₂O₂-using industries such as water and wastewater, pulp and paper, food processing, and animal processing, where waste organics are also produced and/or treated on-site [12–16], and in space missions for life support systems (LSS) where H₂O₂ produced from waste organics could be used for cleaning and disinfection [17].



* Corresponding author.

E-mail address: spopat@clemson.edu (S.C. Popat).

<https://doi.org/10.1016/j.jpowsour.2020.228992>

Received 12 May 2020; Received in revised form 5 September 2020; Accepted 18 September 2020

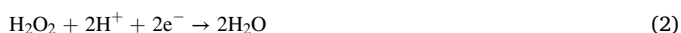
Available online 30 September 2020

0378-7753/© 2020 Published by Elsevier B.V.

In MFCs, waste organics are converted in the anode chamber through a series of microbially-catalyzed reactions under anaerobic conditions to simple fatty acids [18]. Anode-respiring bacteria (ARB) oxidize these simple fatty acids to produce electrical current [19]. At the cathode, O_2 is reduced on inorganic electrocatalysts, most often carbon-based, to H_2O_2 [8,11,20]. To incorporate H_2O_2 production in MFCs, most studies use a cation exchange membrane to separate the anode and the cathode, to avoid exposure of anode microorganisms, especially the ARB, to H_2O_2 , which could be toxic [6,7,10,20]. One alteration however is a single-chambered MFC with H_2O_2 production, which was recently shown to result in better sludge stabilization, without any major effect on the activity of ARB [21].

While precious metal electrocatalysts catalyze the $4-e^-$ O_2 reduction reaction (ORR) to produce water (H_2O), carbon- and non-precious metal-based electrocatalysts are implicated in the $2-e^-$ ORR to produce H_2O_2 [2,22–24]. During the past decade, several new catalysts have been developed and studied for cathodic H_2O_2 electrosynthesis with mesoporous carbon-based electrocatalysts ranking amongst the most efficient [23,25–29]. Although most electrocatalyst development/characterization studies in relation electrosynthesis of H_2O_2 are performed with rotating disk or rotating-ring disk electrodes (RDE or RRDE) in air-saturated solutions, from a scale-up perspective, gas-diffusion electrodes (GDE) provide the most feasible engineering approach, as O_2 can passively diffuse to the electrocatalyst, thus avoiding costs and energy use for aeration [27,30–34]. For GDEs for MFCs, a carbon cloth treated with polytetrafluoroethylene (PTFE), often referred to as a gas-diffusion layer (GDL), to increase its hydrophobicity, is used as the support [35]. Other alternative supports include stainless steel meshes treated in a similar fashion [36]. One side of the support, which faces ambient air, is coated with one or more layers of an ink containing carbon and a hydrophobic polymer (most often PTFE) forming a carbon micro-porous layer (MPL) that allows O_2 diffusion into the GDE, as well as preventing electrolyte leakage [35]. The other side of the support, which faces an electrolyte in which H_2O_2 is collected, is coated with the electrocatalyst ink of interest. The use of GDEs with carbon black electrocatalyst has shown to result in high rates and efficiencies for electrosynthesis of H_2O_2 in MFCs as well as other electrochemical cells [7–11]. Even so, such GDEs are not optimized, like they have been, for example, for proton exchange membrane (PEM) fuel cells.

One outstanding question is how electrocatalyst loading affects the voltage and coulombic efficiency of cathodic electrosynthesis of H_2O_2 on GDEs. Similar studies for PEM fuel cells, have allowed engineering GDEs to have electrocatalyst loadings of as little as 0.1 mg Pt/cm^2 , without compromising on performance [37]. Most electrocatalysts that produce H_2O_2 from the $2-e^-$ ORR will also electrochemically reduce it further to H_2O [24]. Electrocatalyst loading is likely to govern H_2O_2 electrosynthesis by affecting the electrode potential and/or H_2O_2 diffusion within and out of the electrocatalyst layer. In fact, some studies focused on developing non-platinum group metals (non-PGM) as electrocatalysts for the $4-e^-$ ORR have found that electrocatalysts such as cobalt and iron will produce H_2O_2 at high efficiencies, if loaded onto RRDE at low amounts [38–40]. At low loadings of these electrocatalysts, a thin electrocatalyst layer is formed and H_2O_2 diffusion into the electrolyte from the electrocatalyst layer is faster than its electrochemical reduction within the electrocatalyst layer, as per equation (2). Increased loadings lead to a thicker electrocatalyst layer, and H_2O_2 gets reduced in situ faster than its diffusion out of the electrocatalyst layer.



Yet, there is no mechanistic understanding of whether a similar phenomenon of decreased H_2O_2 production with increased electrocatalyst loading occurs on GDEs in which an electrocatalyst ink is applied to a GDL support, the properties of which would affect the electrocatalyst layer properties. Thus, in this study, the effect of loading of carbon black, selected as an electrocatalyst for cathodic

electrosynthesis of H_2O_2 , on GDEs based on a commercially available carbon cloth GDL support was evaluated. To gain mechanistic understanding of the effect of electrocatalyst loading, not only the H_2O_2 production performance, but also how the structure of the GDE and the electrocatalyst layer is altered was studied using scanning electron microscopy (SEM) and X-ray computed tomography (CT) scanning.

2. Materials and methods

2.1. Carbon black electrocatalyst ink

The carbon black electrocatalyst ink used in this study was prepared by first adding and mixing 0.5 g of Vulcan XC 72R carbon black powder (Fuelcellstore.com) and 1 mL of deionized (DI) water in a sterile 20 mL vial. Then, 5 mL of Nafion® D-521 dispersion (5% w/w) (Fuelcellstore.com) was added to the vial, and the mixture was placed in an ultrasonic bath for 30 min to allow for homogenization. The vial was then placed on a magnetic stirrer at a speed of 300 rpm for 24 h to allow the ink to mix before use in preparation of GDEs.

2.2. Gas-diffusion electrodes

To prepare each GDE used in the study, CeTech Carbon Cloth with MPL (Fuelcellstore.com), with dimensions of $6 \text{ cm} \times 6 \text{ cm}$ was first cut out from larger sheets. A square of $5 \text{ cm} \times 5 \text{ cm}$ in the center of cloth was coated with the appropriate amount of carbon black electrocatalyst ink on the side opposite to the MPL. The ink was dispensed by pipetting onto the cloth and then spreading it evenly with a paintbrush. Three carbon black loadings were achieved by using 0.15, 0.45, and 1.0 mL volume of ink for each 25 cm^2 electrode area, corresponding to carbon black loadings of 0.5, 1.5, and 3.33 mg/cm^2 , respectively. The GDEs were allowed to dry overnight after ink application.

2.3. Gas-diffusion half cells

Gas-diffusion half cells were made as previously described in literature [41,42], and shown in Fig. S1 in the Supporting Information, except the anode and cathode chambers were separated by a Chemours Nafion membrane, of $127 \mu\text{m}$ thickness (Fuelcellstore.com). Nafion was chosen as the membrane of choice and it has been found less susceptible to degrade H_2O_2 in a previous studies [9,43]. The volumes of the anode and the cathode chambers were 40 mL and 20 mL respectively. The anode was a hydrophilic carbon cloth (Fuelcellstore.com). The reference electrode used was a RE-5B Ag/AgCl electrode (Bioanalytical Systems, Inc.). For each experiment, the anode and cathode chambers were filled with a 100 mM phosphate buffer solution (PBS) electrolyte containing 35 mM of Na_2HPO_4 and 65 mM of $NaH_2PO_4 \cdot H_2O$, with a pH of 6.45–6.50. The catholyte was continuously mixed by external recirculation at the rate of 25 mL/min.

2.4. GDE performance analysis

A BioLogic VMP3 potentiostat was used for all electrochemical measurements and experiments. Multiple linear sweep voltammograms (LSVs) were performed before beginning each H_2O_2 production test. All LSVs were iR-corrected using either the ZIR or Current Interrupt technique available in the EC-Lab software. After the LSVs were performed, chronopotentiometry method was used to apply constant current to the GDEs. Once a desired current was set, catholyte samples were taken every 30 min. A volume of approximately 0.25 mL was withdrawn at each sampling time point, which allowed for two H_2O_2 concentration measurements at each time point. At the end of each 4-h experiment, the pH of the anolyte and the catholyte was measured. Additionally, the concentration of H_2O_2 in the anode chamber was measured at the end of each experiment; no H_2O_2 was ever detected in the anolyte in any of the experiments performed.

2.5. H_2O_2 measurements

H_2O_2 concentrations in all samples collected were measured using the titanium oxysulfate method [44]. The method involved adding 0.1 mL of samples collected to 1 mL of titanium(IV) oxysulfate-sulfuric acid solution (27–31% H_2SO_4 basis) and 0.9 mL of DI water in a 2 mL plastic cuvette. The titanium(IV) oxysulfate-sulfuric acid solution was sufficiently acidic to protonate any HO_2^- ions; so, this method measured the total concentration of H_2O_2 and HO_2^- in the samples.

2.6. Coulombic efficiency calculations

The coulombic efficiency of H_2O_2 electrosynthesis at each sampling time point was calculated as using equation (3).

$$\text{Coulombic efficiency} = \frac{[H_2O_2] \left(\frac{mg}{L} \right) \times V(L)}{i \text{ (mA)} \times t \text{ (h)} \times 96485 \left(\frac{mC}{mEq} \right) \times 2 \left(\frac{mEq}{mmol} \right) \times 34 \left(\frac{mg}{mmol} \right)} \times 100 \quad (3)$$

Here,

$[H_2O_2]$ = measured H_2O_2 concentration (mg/L) at a given sampling time point

i = current set using chronopotentiometry technique (mA).

t = cumulative time since beginning of experiment at given sampling time point.

2.7. Scanning electron microscopy

All SEM images of GDEs were obtained with a Hitachi S4800 SEM. GDE samples of approximately 2 cm × 2 cm were first clamped between two glass microscope slides, with half of the sample resting in between the slides and half uncovered by the slides. The clamped samples were placed in liquid nitrogen for approximately 10 min. This helped freeze the fibers of the cloth in place so that they did not bend or shift when cut. Then, a razor blade was used to cut off a slice off the piece of the GDEs that was not covered by the glass slides, which was then discarded. The piece of the GDEs that was covered by the glass slides was then mounted on a stub using double sided tape, with the edge that had been sliced with the razor oriented towards the electron beam. This allowed imaging the cross-section of the GDEs and observe distinct layers in the GDE structure. Each sample was imaged at 500X, 1000X, and 2000X.

2.8. X-ray computed tomography

A laboratory X-ray CT system, VECTor⁴CT (MILabs, The Netherlands) was used to obtain 3D reconstructions of all GDEs. Samples for imaging were prepared as 1 cm × 1 cm squares. Each sample was placed between foam in a horizontal tube that was inserted into the CT system. A source voltage of 55 kV and a current of 0.27 mA was used for each sample. A 3D reconstruction of each cathode was performed using ImageJ, using the Volume Viewer plugin. All images were first processed via automatically correcting threshold. To determine the porosity of each GDE, 10 cross-sectional images 10 μ m apart were taken from each 3D reconstructions in the X-Z direction. These images were further processed using MATLAB. Carbon within each image was set to appear as pink, and empty pore space was set to appear as black, and a MATLAB code was developed to count the number of pink and black pixels within each image. The porosity of each GDE was then calculated as the average of the 10 values.

3. Results and discussion

3.1. Electrochemical characterization gas-diffusion electrodes with different carbon black loadings

First, to determine if the different carbon black loadings on GDEs for H_2O_2 production lead to different polarization curves for the GDEs, cathodic LSVs were obtained for each of the different GDEs, in 100 mM PBS electrolyte at pH ~6.45–6.5. The electrolyte chosen here was on the basis of typical conditions anticipated to be used in biological fuel cells such as MFCs for H_2O_2 production [41]. Discussed later is how the choice of pH may affect H_2O_2 production on GDEs. Multiple LSVs were obtained for each GDE and shown in Fig. 1 are select representative LSVs. All LSVs are iR-corrected. The ohmic resistance determined for each scan for the different GDEs were similar, and thus did not point to any major changes in electrode electrical conductivity with changes in carbon black loading. Also shown in Fig. 1 with a dotted line is the theoretical potential for H_2O_2 production from ORR at a pH of 7 (~+0.3 V vs. SHE). From Fig. 1, it is obvious that adding carbon black as an electrocatalyst significantly improves the ORR kinetics. For example, at a current density of 1 mA/cm², the overpotential for the CeTech Carbon Cloth with MPL, i.e. without any electrocatalyst, and referred to as bare GDL is ~1.05 V while for the GDEs with the carbon black electrocatalyst is 0.3–0.4 V. Considering this, all H_2O_2 production experiments described hereon focus only on the three carbon black electrocatalyst loadings, and not on the bare GDL.

Between the different carbon black loadings, no major differences in the LSVs are noted at high current densities (>1 mA/cm²). Additionally, no O_2 limitation, usually characterized by a sharp overpotential at high current densities, was observed at least until current densities of 5 mA/cm², suggesting that the different carbon black loadings do not affect O_2 diffusion in the electrocatalyst layer enough to lead to O_2 limitation at the range of current densities used in the study. At lower current densities (<1 mA/cm²) and at open circuit, some differences can be observed. First, the open circuit voltages (OCVs) for each of the three carbon black loadings differed, with increasing OCVs resulting from increasing carbon black loadings. The theoretical potential for H_2O_2 production from ORR is ~+0.3 V vs. SHE, and yet all of the OCVs were higher. The theoretical potential for the 4-e⁻ ORR at neutral pH is ~+0.81 V vs. SHE, and so it appears that the OCVs here represent a mixed potential, with some potential for catalyzing the 4-e⁻ ORR on each of the GDEs with the different carbon black loadings. A higher OCV for

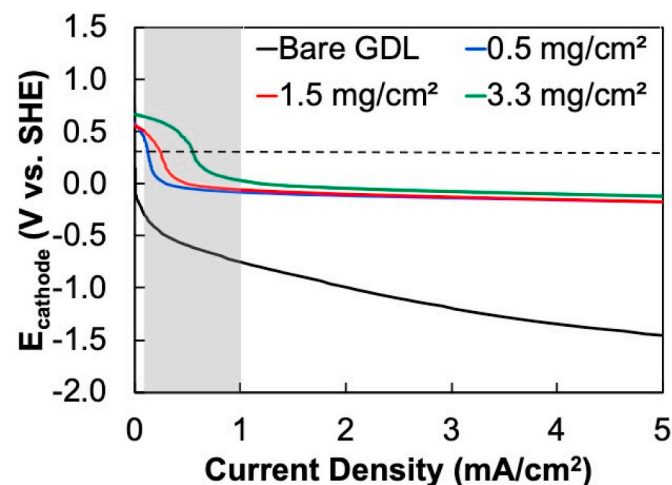


Fig. 1. Linear sweep voltammograms of GDEs with different loadings of Vulcan carbon XC 72R as the electrocatalyst. Bare GDL represents a control with no electrocatalyst loading. A total of 10 voltammograms were recorded for each GDE and shown here is one representative. Shaded in grey is the range of current densities that was used for the H_2O_2 production experiments.

the highest carbon black loadings thus also indicates a higher potential for the 4-e⁻ ORR, which could potentially lead to lower H₂O₂ production efficiency, depending on the current density.

Shown in Fig. 1 highlighted in grey is the range of current densities that was used for the H₂O₂ production experiments described below. This range is not only where some differences are noted in the LSVs, but also is representative of a typical range of current densities obtained in MFCs [45], as well as other biological fuel cells [46], where H₂O₂ production could be incorporated.

3.2. H₂O₂ production comparison for gas-diffusion electrodes with different carbon black loadings

Shown in Fig. 2 are results from the H₂O₂ electrosynthesis experiments conducted for the GDEs with the different carbon black loadings. Fig. 2a, b and 2c show the concentration of H₂O₂ accumulated in the cathode chamber of the gas-diffusion half-cells during a 4-h batch experiments at three different current densities (0.1, 0.5 and 1.0 mA/cm²), while Fig. 2d, e, and 2f show the corresponding cathodic coulombic efficiencies. From Fig. 2, several observations can be made. First, irrespective of the current density, the GDEs with a carbon loading of 3.3 mg/cm² consistently underperformed in terms of H₂O₂ production, with a 4-h coulombic efficiency of $12.4 \pm 0.7\%$, $19.5 \pm 5.4\%$ and $20.6 \pm 0.7\%$ at current densities of 0.1, 0.5 and 1.0 mA/cm² respectively. In comparison, carbon black loadings of 0.5 and 1.5 mg/cm² resulted in similar

coulombic efficiencies at 4 h of $27.3 \pm 0.6\%$, $47.7 \pm 3.2\%$, and $25.6 \pm 3.5\%$ at current densities of 0.1, 0.5 and 1.0 mA/cm² respectively for 0.5 mg/cm² loading and $29.7 \pm 3.8\%$, $42.0 \pm 2.9\%$, and $27.3 \pm 0.6\%$ at current densities of 0.1, 0.5 and 1.0 mA/cm² respectively for 1.5 mg/cm² loading. Such a decrease in coulombic efficiency with increasing electrocatalyst loading has been observed previously in RRDE experiments not only with carbon black electrocatalysts, but other electrocatalysts as well, including PGM electrocatalysts, as well as non-PGM electrocatalysts including cobalt and iron [38–40]. In these studies, the decrease in efficiency is clearly linked to an increased electrocatalyst layer thickness that likely leads to diffusional limitations for H₂O₂, and its further reduction in situ in the electrocatalyst layer. However, the question that arises is if the mechanism of the efficiency decrease is the same on GDEs as RRDEs. Understanding the mechanism of this phenomenon will lead to new avenues to fabrication of GDEs with properties more suitable for enhancing H₂O₂ diffusion out of the electrocatalyst layer. This is addressed later through detailed structural analysis of the GDEs prepared here.

Second, for the highest current density tested, of 1 mA/cm², a significant decrease in coulombic efficiency can be noted after an experimental duration of 2–3 h, especially for the carbon black loadings of 0.5 and 1.5 mg/cm². H₂O₂ concentrations in this case increase linearly to 946 ± 17 mg/L for 0.5 mg/cm² loading at 2.5 h and to 1035 ± 29 mg/L for 1.5 mg/cm² loading at 3 h, and then plateau for the rest of the experimental duration. This efficiency decrease is postulated to be a

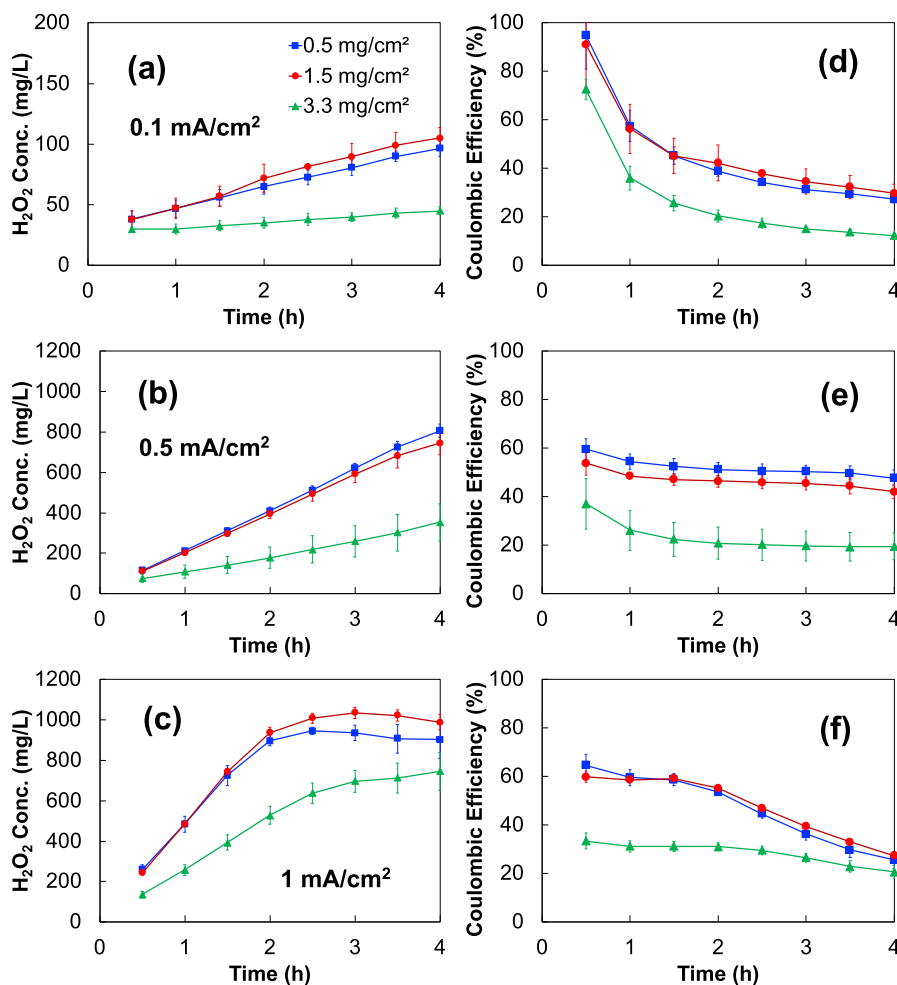


Fig. 2. (a, b, and c) H₂O₂ concentrations, and (d, e, and f) coulombic efficiency, achieved using GDEs with different loadings of Vulcan carbon XC 72R as the electrocatalyst, in a 4-h batch test at three different current densities. Each experiment was repeated thrice, and data reported is an average of triplicate experiments. Error bars show the standard deviation.

result of an increase in cathode pH to >10 . Shown in Fig. 3 are the cathode pH values at the end of the each of the experiments, as a function of the current density. A higher current density leads to an increase in the cathode pH, because of the larger consumption of protons or the production of hydroxide ions during the $2e^-$ -ORR. Shown in Fig. 3, shaded in grey, is also the range of pH values in which the H_2O_2/HO_2^- ratio changes from 99/1 to 1/99; this occurs due to the deprotonation of H_2O_2 as per equation (4). HO_2^- is more unstable than H_2O_2 , with rates of auto-degradation significantly higher [47]. If the cathode pH thus increases to well above 10, significant coulombic efficiency decreases can be expected as H_2O_2 deprotonates to the unstable HO_2^- .



Higher cathode pH values at 1 mA/cm^2 in comparison to the 0.1 and 0.5 mA/cm^2 thus support the decreasing coulombic efficiency, especially for carbon black loadings of 0.5 and 1.5 mg/cm^2 . For the intermediate current density of 0.5 mA/cm^2 , a slight downward trend in coulombic efficiency appears to exist at the end of the 4-h experiment, especially for carbon black loadings of 0.5 and 1.5 mg/cm^2 , as the pH increases to just above 10. Even so, it is also important to note that the cathode pH was lower in the carbon black loading of 3.33 mg/cm^2 compared to the other carbon black loadings despite the same current density at both 0.5 and 1 mA/cm^2 ; this could be a result of slower OH^- ion diffusion out of the less porous electrocatalyst layer. This translates to a smaller (or no) decrease in coulombic efficiency with time, despite a lower overall coulombic efficiency in comparison to the other two carbon black loadings.

For the current density of 0.1 mA/cm^2 , a sharp decrease in coulombic efficiency is noted from the first sampling point onwards. However, this cannot be related to the cathode pH, as even at the end of each experiment, the cathode pH at the lowest current densities, irrespective of the carbon black loading, was <7 . This decrease in coulombic efficiency is likely governed by other phenomena, which could most likely be electrochemical reduction of H_2O_2 at the electrode potentials attained at the lower current densities to H_2O [48]. However, without further tests in the present set-up with the as-fabricated GDEs, it is not possible to confirm this hypothesis.

Even so, the observation that cathode pH has a significant impact of coulombic efficiency in cathodic H_2O_2 production has several implications for H_2O_2 production in biological fuel cells, including MFCs, which are often operated at physiological pHs [45]. The increase in pH in the present experiments to >10 , with a corresponding decrease in

coulombic efficiency, suggests that H_2O_2 production at pH values of 10–12 should be the most impacted. Above a pH of 12, many metal impurities that may be present in the catholyte likely will precipitate out, thus improving the stability of HO_2^- . This should be evaluated in further studies with GDEs, along with a wide range of catholyte pHs, and the effects of hydrodynamics on changes in catholyte pH. Most of the existing literature on cathodic H_2O_2 production has focused exclusively on acidic or basic pHs, to study the selectivity of several catalysts under the two extreme conditions [4,5,49]. Studies on neutral pH electrochemical production of H_2O_2 are fewer and have not elaborated on the effect of increasing cathode pH on coulombic efficiency [50–52]. However, to make H_2O_2 production feasible in MFCs, it is essential to understand this relationship, and study methods with an increase in cathode pH can be hindered, to allow for high coulombic efficiencies. To illustrate the effect that a lack in cathode pH increase would have, we performed H_2O_2 production tests with a carbon black loading of 1.5 mg/cm^2 in 500 mM PBS as well and compared the results to those in 100 mM PBS, for a current density of 1 mA/cm^2 . The results from these are shown in Fig. S2 in the Supporting Information. When using a 500 mM PBS catholyte, cathode pH increased only to 7.10 from 6.50, compared to 10.70 with 100 mM PBS catholyte, and correspondingly there was no decrease in coulombic efficiency throughout the 4-h production experiments, with H_2O_2 concentrations accumulated to as high as 2000 mg/L. The effect of electrolyte pH on H_2O_2 production should be a topic of further study, especially as using high buffer concentrations is not feasible for practical applications.

3.3. Characterization of structures of gas-diffusion electrodes with different carbon black electrocatalyst loadings

Shown in Fig. 4 are SEM micrographs of the various GDEs prepared with different carbon black electrocatalyst loadings; Fig. 4a is a cross-section of a GDE with 3.3 mg/cm^2 carbon black loading, while Fig. 4b shows zoomed in portions of the cross-section of each of the three GDEs with the different carbon black loadings (0.5, 1.5 and 3.3 mg/cm^2), as well as a bare GDL. From Fig. 4a, it becomes apparent that rather than forming a distinct electrocatalyst layer on top of the carbon cloth support, the method of electrocatalyst layer preparation used in this study, viz. brush-painting, in combination with the properties of the carbon cloth support used, likely resulted in carbon black becoming embedded in the carbon cloth support. In Fig. 4a, the carbon MPL of the support can be clearly seen at the bottom end of the GDE as a backing to the carbon cloth structure.

For PEM fuel cells, GDEs are prepared either with the carbon MPL facing the air side or the membrane side, with distinct advantages noted for each approach [53,54]. In the case of fuel cells with aqueous electrolytes however, such as MFCs, it is common to include a carbon MPL on the air side rather than the electrolyte side [35], as is the case also in this study. This configuration allows altering the air-facing side with multiple coatings of the MPL to avoid electrolyte leakage, if necessary. Whether or not the catalyst ink application would lead to a distinct electrocatalyst layer formation on top of the carbon cloth depends on the hydrophobicity of the carbon cloth, and in the case here, CeTech carbon cloth with a 30% PTFE loading was not hydrophobic enough to allow for carbon black to be loaded on top of the carbon cloth, forming a distinct electrocatalyst layer. Rather the carbon black embedded within the carbon cloth for each of the carbon black loadings tested, as is apparent in Fig. 4b. Fig. 4b also indicates that increasing the carbon black loading likely results in decreasing porosity of the carbon cloth with more carbon black coating each of the carbon fibers of the carbon cloth. This makes the carbon cloth layer of the GDE analogous to the electrocatalyst layer. Fig. S3 and S4 in the Supporting Information show more SEM micrographs with different zoom levels, supporting the hypothesis here of a decreased porosity of the electrocatalyst layer with increasing carbon black loading.

In RRDE studies focused on evaluating the effect of electrocatalyst

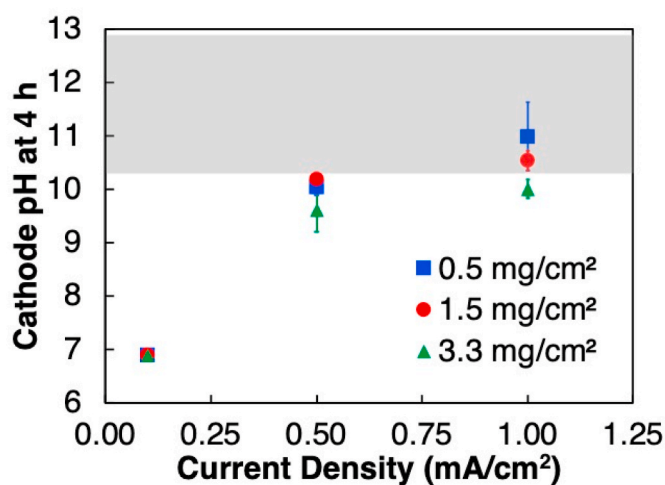


Fig. 3. Final catholyte pHs at the end of 4-h batch chronopotentiometry experiments. All reported average values are based on experiments repeated thrice. Error bars show the standard deviation. Shaded in grey the range of pH values in which the H_2O_2/HO_2^- ratio changes from 99/1 to 1/99.

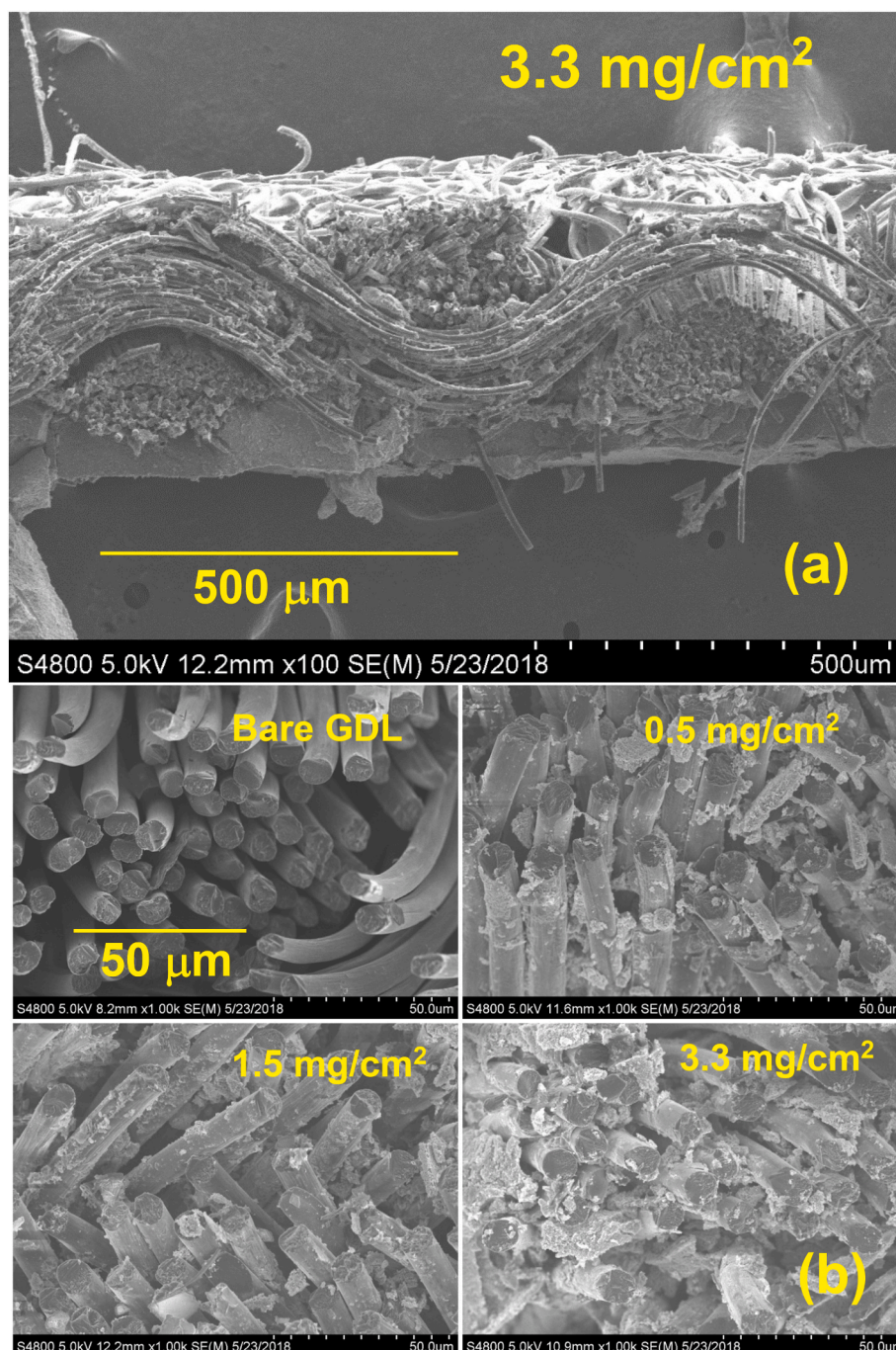


Fig. 4. Scanning electron microscopy (SEM) images of cross-sections GDEs with different loadings of Vulcan carbon XC 72R as the electrocatalyst. Bare GDL represents a control with no electrocatalyst loading. Samples were imaged at 1000X.

loading on ORR, an increased thickness of the electrocatalyst layer with increasing electrocatalyst loading has been noted [38–40], as discussed before. Instead, here, on a commercially available carbon cloth support, it is observed that rather than altering the electrocatalyst layer thickness, increased catalyst loading leads to a decreased porosity of the electrocatalyst layer. This decreased electrocatalyst layer porosity likely leads to the same effects on the ORR as noted in RRDE studies with increased electrocatalyst layer thickness, viz. transition from 2- e^- ORR to 4- e^- ORR, due to in situ reduction of H_2O_2 , stemming from diffusional limitations.

For further qualitative evaluation of the change in electrocatalyst layer porosity with increasing carbon black loading, X-ray CT 3D reconstructions of the GDEs with the different carbon black loadings were

obtained. In Fig. 5, cross-sections showing 3D reconstructions of each of the GDEs are shown. In the figure, pink color indicates the location of all carbon that can be detected using X-ray measurements. Note that it was not possible to distinguish between the carbon black electrocatalyst, the carbon cloth support and the carbon MPL using the image-processing techniques used here, and so the pink color constitutes the composite GDE. It is, however, easily confirmed from Fig. 5 that increasing carbon black loading leads to a denser, less porous electrocatalyst layer, as previously indicated by the SEM micrographs.

To obtain quantitative information on changes in porosity of the electrocatalyst layer resulting from the increased carbon black loadings, the X-ray CT 3D reconstructions were processed into multiple slices of the GDEs that were then filtered using a MATLAB code as described in

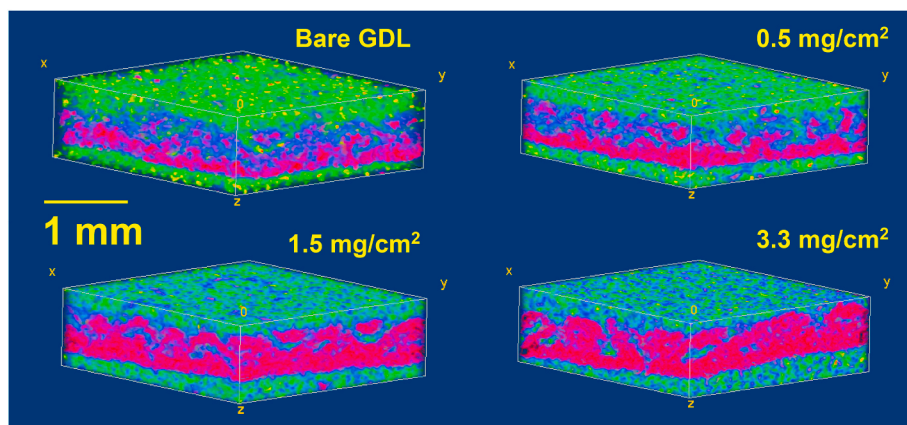


Fig. 5. X-ray CT reconstructions of GDEs with different loadings of Vulcan carbon XC 72R as the electrocatalyst. Bare GDL represents a control with no electrocatalyst loading. Shown are reconstructions of a 1 mm × 1 mm section of each of the GDEs, as processed using ImageJ, with pink color denoting carbon. No distinction could be made between Vulcan carbon XC 72R, and carbon fibers of the CeTech carbon cloth GDL. (For interpretation of the references to color in this figure legend, the reader is referred to the Web version of this article.)

the materials and methods section, to allow for determination of overall GDE porosity (Fig. S5 in the Supporting Information). These determinations are shown in Table 1, from which it is clear that substantial decrease in overall GDE porosity occurs as a result of increasing carbon black loading, with a marked decrease noted when loading is increased from 1.5 to 3.3 mg/cm². Another important observation from the slides of GDE shown in Fig. S5 and from the small standard deviations in the porosity calculated is the uniformity of the catalyst ink application. Due to a lower resolution offered from a micro-CT scanner used here compared to a nano-CT scanner that is used in some recent studies to determine gas-diffusion layer porosities [55], it was not possible to distinguish the porosities of the electrocatalyst layer from the carbon MPL, and thus the porosities reported in Table 1 are useful only for relative comparison, but are not the absolute porosities of the electrocatalyst layer resulting from different carbon black loadings.

Overall, the structural characterization of the GDEs, using a combination of SEM micrographs and X-ray CT 3D reconstructions, confirms both qualitatively and semi-quantitatively that increased carbon black loading leads to a decreased porosity of the electrocatalyst layer on the carbon cloth support used here. This decreased porosity corresponds directly with a decreasing efficiency of H₂O₂ electrosynthesis in experiments shown in Fig. 2.

3.4. Perspectives on gas-diffusion electrode development for H₂O₂ production

Considering the strong effect the carbon black catalyst loading had in the present experiments on the cathodic coulombic efficiency in H₂O₂ production, and the likely mechanism of decrease in efficiency through H₂O₂ diffusion limitations along with electrochemical and/or chemical decomposition in situ in the electrocatalyst layer, it can be deduced that the best electrocatalyst configuration for GDEs for cathodic H₂O₂ production would be a thin layer which limits the reaction to the electrolyte-electrode interface. This could potentially be achieved with

tuning the hydrophobicity of the electrocatalyst layer to block water diffusion beyond the interface. To test this hypothesis, we used the CeTech carbon cloth with MPL (i.e. the bare GDL), with the MPL facing the electrolyte, as the electrocatalyst, and compared the performance in terms of coulombic efficiency to the carbon black loading of 1.5 mg/cm². The MPL for this GDL is synthesized with carbon black mixed with PTFE which makes the layer significantly hydrophobic.

Shown in Fig. 6 is the comparison of the carbon MPL electrocatalyst against the 1.5 mg/cm² carbon black electrocatalyst loading for H₂O₂ electrosynthesis at a current density of 1 mA/cm². As hypothesized, the carbon MPL produced H₂O₂ to higher concentrations and with higher coulombic efficiency. H₂O₂ concentrations with the carbon MPL electrocatalyst increased to 1314 ± 51 mg/L, compared to ~1035 ± 29 mg/L on the 1.5 mg/cm² carbon black electrocatalyst. Even so an increasing catholyte pH (>10) led to a decrease in efficiency beyond 2 h, as with the previous experiments described. While the purpose of this experiment was not to advocate the use of the carbon MPL as the electrocatalyst for H₂O₂ production, the results obtained do warrant studying tuning electrocatalyst layer hydrophobicity as a method to improve performance of H₂O₂-producing GDEs through limiting the electrochemical reactions to electrocatalyst area that does not limit H₂O₂ diffusion into the electrolyte.

4. Conclusions

In this study, the effect of carbon black electrocatalyst loading on GDEs for H₂O₂ electrosynthesis in neutral catholytes, for possible use in MFCs, was studied. Higher carbon black loading (3.3 mg/cm² vs. 0.5 and 1 mg/cm²) did not provide any benefits in terms of electrochemical performance. However, higher loading did lead to a lower cathodic coulombic efficiency. At the end of 4-h batch electrosynthesis experiment, the coulombic efficiency for a carbon black loading of 3.3 mg/cm² ranged between 12 and 21% depending on the current density, while for smaller loadings, ranged between 25 and 48%. This decrease in efficiency as a result of increasing carbon black loading was attributed to a decreased GDE porosity, resulting in mass transport limitations for H₂O₂ out of the GDE. Under mass transport limiting conditions, H₂O₂ is likely consumed in-situ in the GDE through electrochemical reduction, or auto-degradation at a high pH.

CRediT authorship contribution statement

Emily Murawski: Conceptualization, Methodology, Investigation, Writing - original draft, Visualization. **Negin Kananizadeh:** Investigation, Data curation, Visualization. **Spencer Lindsay:** Investigation, Visualization. **Apparao M. Rao:** Writing - review & editing. **Sudeep C. Popat:** Conceptualization, Methodology, Writing - original draft, Writing - review & editing, Visualization, Supervision, Funding

Table 1

Porosities of GDEs calculated using 10 sections from X-ray CT reconstructions of each GDE with different loadings of Vulcan carbon XC 72R electrocatalyst. To determine porosity, each section sliced using ImageJ was processed using a MATLAB code developed to determine porosity. Porosity calculations are for the entire GDE including the carbon MPL, as resolution available did not allow clearly delineating the different layers in the GDEs.

	Gas-diffusion electrode porosity (%)
Bare GDL	66.9 ± 0.7
0.5 mg/cm ²	40.7 ± 1.3
1.5 mg/cm ²	38.0 ± 1.3
3.3 mg/cm ²	31.8 ± 0.4

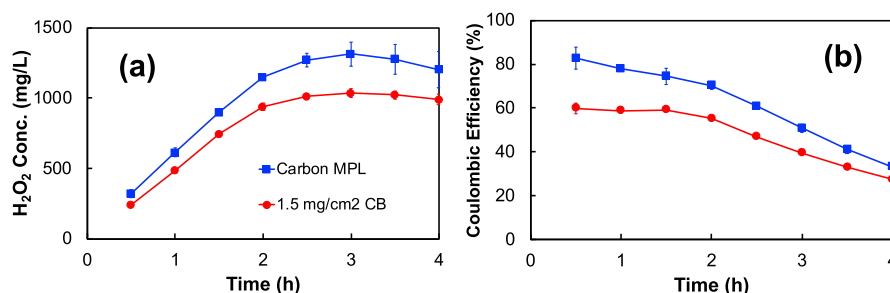


Fig. 6. (a) H₂O₂ concentrations, and (b) coulombic efficiency, achieved using GDEs of 1.5 mg/cm² carbon black electrocatalyst vs. a carbon MPL electrocatalyst, in a 4-h batch test at a current density of 1 mA/cm². Each experiment was repeated thrice, and data reported is an average of triplicate experiments. Error bars show the standard deviation.

acquisition.

Declaration of competing interest

The authors declare that they have no known competing financial interests or personal relationships that could have appeared to influence the work reported in this paper.

Acknowledgments

The authors acknowledge the assistance of Dr. Brian Powell, Megha Patel and Nicholas Mitchell in performing X-ray CT scanning and image processing of the 3D reconstructions using ImageJ, and of George Wetzel in performing SEM imaging. The authors also acknowledge the South Carolina Space Grant Consortium, the NASA EPSCoR program, and the Fats and Proteins Research Foundation through the ACREC program at Clemson, for providing funding.

Appendix A. Supplementary data

Supplementary data related to this article can be found at <https://doi.org/10.1016/j.jpowsour.2020.228992>.

References

- J.M. Campos-Martin, G. Blanco-Brieva, J.L.G. Fierro, Hydrogen peroxide synthesis: an outlook beyond the anthraquinone process, *Angew. Chem. Int. Ed.* 45 (2006) 6962–6984, <https://doi.org/10.1002/anie.200503779>.
- M. Melchionna, P. Fornasiero, M. Prato, The rise of hydrogen peroxide as the main product by metal-free catalysis in oxygen reductions, *Adv. Mater.* 31 (2019) 1802920, <https://doi.org/10.1002/adma.201802920>.
- K. Otsuka, I. Yamanaka, One step synthesis of hydrogen peroxide through fuel cell reaction, *Electrochim. Acta* 35 (1990) 319–322, [https://doi.org/10.1016/0013-4686\(90\)87004-L](https://doi.org/10.1016/0013-4686(90)87004-L).
- I. Yamanaka, T. Onizawa, S. Takenaka, K. Otsuka, Direct and continuous production of hydrogen peroxide with 93 % selectivity using a fuel-cell system, *Angew. Chem. Int. Ed.* 42 (2003) 3653–3655, <https://doi.org/10.1002/anie.200351343>.
- I. Yamanaka, T. Onisawa, T. Hashimoto, T. Murayama, A fuel-cell reactor for the direct synthesis of hydrogen peroxide alkaline solutions from H₂ and O₂, *ChemSusChem* 4 (2011) 494–501, <https://doi.org/10.1002/cssc.201000263>.
- L. Fu, S.-J. You, F. Yang, M. Gao, X. Fang, G. Zhang, Synthesis of hydrogen peroxide in microbial fuel cell, *J. Appl. Chem. Biotechnol.* 85 (2010) 715–719, <https://doi.org/10.1002/jctb.2367>.
- J.B.A. Arends, S. Van Denhouwe, W. Verstraete, N. Boon, K. Rabaey, Enhanced disinfection of wastewater by combining wetland treatment with bioelectrochemical H₂O₂ production, *Bioresour. Technol.* 155 (2014) 352–358, <https://doi.org/10.1016/j.biortech.2013.12.058>.
- R.A. Rozendal, E. Leone, J. Keller, K. Rabaey, Efficient hydrogen peroxide generation from organic matter in a bioelectrochemical system, *Electrochem. Commun.* 11 (2009) 1752–1755, <https://doi.org/10.1016/j.elecom.2009.07.008>.
- M.N. Young, M.J. Links, S.C. Papat, B.E. Rittmann, C.I. Torres, Tailoring microbial electrochemical cells for production of hydrogen peroxide at high concentrations and efficiencies, *ChemSusChem* 9 (2016) 3345–3352, <https://doi.org/10.1002/cssc.201601182>.
- J. Chen, N. Li, L. Zhao, Three-dimensional electrode microbial fuel cell for hydrogen peroxide synthesis coupled to wastewater treatment, *J. Power Sources* 254 (2014) 316–322, <https://doi.org/10.1016/j.jpowsour.2013.12.114>.
- M.N. Young, N. Chowdhury, E. Garver, P.J. Evans, S.C. Papat, B.E. Rittmann, C. I. Torres, Understanding the impact of operational conditions on performance of microbial peroxide producing cells, *J. Power Sources* 356 (2017) 448–458, <https://doi.org/10.1016/j.jpowsour.2017.03.107>.
- W.H. Glaze, J.-W. Kang, D.H. Chapin, The chemistry of water treatment processes involving ozone, hydrogen peroxide and ultraviolet radiation, *Ozone: Sci. Eng.* 9 (1987) 335–352, <https://doi.org/10.1080/01919518708552148>.
- M. Ksibi, Chemical oxidation with hydrogen peroxide for domestic wastewater treatment, *Chem. Eng. J.* 119 (2006) 161–165, <https://doi.org/10.1016/j.cej.2006.03.022>.
- S. Camarero, D. Ibarra, Á.T. Martínez, J. Romero, A. Gutiérrez, J.C. del Río, Paper pulp delignification using laccase and natural mediators, *Enzym. Microb. Technol.* 40 (2007) 1264–1271, <https://doi.org/10.1016/j.enzmictec.2006.09.016>.
- M. Elleuch, D. Bedigian, O. Roiseux, S. Besbes, C. Blecker, H. Attia, Dietary fibre and fibre-rich by-products of food processing: characterisation, technological functionality and commercial applications: a review, *Food Chem.* 124 (2011) 411–421, <https://doi.org/10.1016/j.foodchem.2010.06.077>.
- I.A. Pettas, M.I. Karayannis, Simultaneous spectra-kinetic determination of peracetic acid and hydrogen peroxide in a brewery cleaning-in-place disinfection process, *Anal. Chim. Acta* 522 (2004) 275–280, <https://doi.org/10.1016/j.aca.2004.07.010>.
- T. Pottage, S. Macken, K. Giri, J.T. Walker, A.M. Bennett, Low-temperature decontamination with hydrogen peroxide or chlorine dioxide for space applications, *Appl. Environ. Microbiol.* 78 (2012) 4169–4174, <https://doi.org/10.1128/AEM.07948-11>.
- H. Liu, R. Ramnarayanan, B.E. Logan, Production of electricity during wastewater treatment using a single chamber microbial fuel cell, *Environ. Sci. Technol.* 38 (2004) 2281–2285, <https://doi.org/10.1021/es034923g>.
- C.I. Torres, A. Kato Marcus, B.E. Rittmann, Kinetics of consumption of fermentation products by anode-respiring bacteria, *Appl. Microbiol. Biotechnol.* 77 (2007) 689–697, <https://doi.org/10.1007/s00253-007-1198-z>.
- D. Ki, S.C. Papat, B.E. Rittmann, C.I. Torres, H₂ O₂ production in microbial electrochemical cells fed with primary sludge, *Environ. Sci. Technol.* 51 (2017) 6139–6145, <https://doi.org/10.1021/acs.est.7b00174>.
- D. Ki, R. Kupferer, C.I. Torres, High-rate stabilization of primary sludge in a single-chamber microbial hydrogen peroxide producing cell, *Environ. Sci. J. Integr. Environ. Res.: Water Research & Technology* 5 (2019) 1124–1131, <https://doi.org/10.1039/C9EW00100J>.
- J.M. Campos-Martin, G. Blanco-Brieva, J.L.G. Fierro, Hydrogen peroxide synthesis: an outlook beyond the anthraquinone process, *Angew. Chem. Int. Ed.* 45 (2006) 6962–6984, <https://doi.org/10.1002/anie.200503779>.
- S. Chen, Z. Chen, S. Siahrostami, T.R. Kim, D. Nordlund, D. Sokaras, S. Nowak, J. W.F. To, D. Higgins, R. Sinclair, J.K. Nørskov, T.F. Jaramillo, Z. Bao, Defective carbon-based materials for the electrochemical synthesis of hydrogen peroxide, *ACS Sustain. Chem. Eng.* 6 (2018) 311–317, <https://doi.org/10.1021/acssuschemeng.7b02517>.
- W.P. Mounfield, A. Garg, Y. Shao-Horn, Y. Román-Leshkov, Electrochemical oxygen reduction for the production of hydrogen peroxide, *Inside Chem.* 4 (2018) 18–19, <https://doi.org/10.1016/j.chempr.2017.12.015>.
- T.-P. Fellinger, F. Hasché, P. Strasser, M. Antonietti, Mesoporous nitrogen-doped carbon for the electrocatalytic synthesis of hydrogen peroxide, *J. Am. Chem. Soc.* 134 (2012) 4072–4075, <https://doi.org/10.1021/ja300038p>.
- Z. Lu, G. Chen, S. Siahrostami, Z. Chen, K. Liu, J. Xie, L. Liao, T. Wu, D. Lin, Y. Liu, T.F. Jaramillo, J.K. Nørskov, Y. Cui, High-efficiency oxygen reduction to hydrogen peroxide catalysed by oxidized carbon materials, *Nature Catalysis* 1 (2018) 156–162, <https://doi.org/10.1038/s41929-017-0017-x>.
- G.A. Kolyagin, G.V. Kornienko, V.L. Kornienko, I.V. Ponomarenko, Electrochemical reduction of oxygen to hydrogen peroxide in a gas-diffusion electrode based on mesoporous carbon, *Russ. J. Appl. Chem.* 90 (2017) 1143–1147, <https://doi.org/10.1134/S1070427217070187>.
- H.W. Kim, M.B. Ross, N. Kornienko, L. Zhang, J. Guo, P. Yang, B.D. McCloskey, Efficient hydrogen peroxide generation using reduced graphene oxide-based oxygen reduction electrocatalysts, *Nature Catalysis* 1 (2018) 282–290, <https://doi.org/10.1038/s41929-018-0044-2>.
- N. Li, J. An, L. Zhou, T. Li, J. Li, C. Feng, X. Wang, A novel carbon black graphite hybrid air-cathode for efficient hydrogen peroxide production in

- bioelectrochemical systems, *J. Power Sources* 306 (2016) 495–502, <https://doi.org/10.1016/j.jpowsour.2015.12.078>.
- [30] W.R.P. Barros, T. Ereno, A.C. Tavares, M.R.V. Lanza, In situ electrochemical generation of hydrogen peroxide in alkaline aqueous solution by using an unmodified gas diffusion electrode, *ChemElectroChem* 2 (2015) 714–719, <https://doi.org/10.1002/celec.201402426>.
- [31] V.L. Kornienko, G.A. Kolyagin, G.V. Kornienko, V.A. Parfenov, I.V. Ponomarenko, Electrosynthesis of H₂O₂ from O₂ in a gas-diffusion electrode based on mesostructured carbon CMK-3, *Russ. J. Electrochem.* 54 (2018) 258–264, <https://doi.org/10.1134/S1023193518030060>.
- [32] H. Luo, C. Li, C. Wu, X. Dong, In situ electrosynthesis of hydrogen peroxide with an improved gas diffusion cathode by rolling carbon black and PTFE, *RSC Adv.* 5 (2015) 65227–65235, <https://doi.org/10.1039/C5RA09636G>.
- [33] R.M. Reis, A.A.G.F. Beati, R.S. Rocha, M.H.M.T. Assumpção, M.C. Santos, R. Bertazzoli, M.R.V. Lanza, Use of gas diffusion electrode for the in situ generation of hydrogen peroxide in an electrochemical flow-by reactor, *Ind. Eng. Chem. Res.* 51 (2012) 649–654, <https://doi.org/10.1021/ie201317u>.
- [34] R.B. Valim, R.M. Reis, P.S. Castro, A.S. Lima, R.S. Rocha, M. Bertotti, M.R.V. Lanza, Electrogeneration of hydrogen peroxide in gas diffusion electrodes modified with tert-butyl-anthraquinone on carbon black support, *Carbon* 61 (2013) 236–244, <https://doi.org/10.1016/j.carbon.2013.04.100>.
- [35] S. Cheng, H. Liu, B.E. Logan, Increased performance of single-chamber microbial fuel cells using an improved cathode structure, *Electrochem. Commun.* 8 (2006) 489–494, <https://doi.org/10.1016/j.elecom.2006.01.010>.
- [36] S. Chen, Y. Chen, G. He, S. He, U. Schröder, H. Hou, Stainless steel mesh supported nitrogen-doped carbon nanofibers for binder-free cathode in microbial fuel cells, *Biosens. Bioelectron.* 34 (2012) 282–285, <https://doi.org/10.1016/j.bios.2011.10.049>.
- [37] Z. Qi, A. Kaufman, Low Pt loading high performance cathodes for PEM fuel cells, *J. Power Sources* 113 (2003) 37–43, [https://doi.org/10.1016/S0378-7753\(02\)00477-9](https://doi.org/10.1016/S0378-7753(02)00477-9).
- [38] E.J. Biddinger, D. von Deak, D. Singh, H. Marsh, B. Tan, D.S. Knapke, U.S. Ozkan, Examination of catalyst loading effects on the selectivity of CN_x and Pt/VC ORR catalysts using RRDE, *J. Electrochem. Soc.* 158 (2011) B402, <https://doi.org/10.1149/1.3552944>.
- [39] X. Li, H.-J. Zhang, H. Li, C. Deng, J. Yang, Evaluation of loading influence on catalytic performance of Co-based catalyst for oxygen reduction, *ECS Electrochemistry Letters* 3 (2014) H33–H37, <https://doi.org/10.1149/2.0061409eel>.
- [40] A. Bonakdarpour, M. Lefevre, R. Yang, F. Jaouen, T. Dahn, J.-P. Dodelet, J.R. Dahn, Impact of loading in RRDE experiments on Fe–N–C catalysts: two- or four-electron oxygen reduction? *Electrochem. Solid State Lett.* 11 (2008) B105, <https://doi.org/10.1149/1.2904768>.
- [41] S.C. Popat, D. Ki, B.E. Rittmann, C.I. Torres, Importance of OH[−] transport from cathodes in microbial fuel cells, *ChemSusChem* 5 (2012) 1071–1079, <https://doi.org/10.1002/cssc.201100777>.
- [42] S.C. Popat, D. Ki, M.N. Young, B.E. Rittmann, C.I. Torres, Buffer pK_a and transport govern the concentration overpotential in electrochemical oxygen reduction at neutral pH, *ChemElectroChem* 1 (2014) 1909–1915, <https://doi.org/10.1002/celec.201402058>.
- [43] T. Kinumoto, M. Inaba, Y. Nakayama, K. Ogata, R. Umebayashi, A. Tasaka, Y. Iriyama, T. Abe, Z. Ogumi, Durability of perfluorinated ionomer membrane against hydrogen peroxide, *J. Power Sources* 158 (2006) 1222–1228, <https://doi.org/10.1016/j.jpowsour.2005.10.043>.
- [44] G. Eisenberg, Colorimetric Determination of Hydrogen Peroxide, (n.d.) vol. 2.
- [45] C. Santoro, C. Arbizzani, B. Erable, I. Ieropoulos, Microbial fuel cells: from fundamentals to applications. A review, *J. Power Sources* 356 (2017) 225–244, <https://doi.org/10.1016/j.jpowsour.2017.03.109>.
- [46] S. Cosnier, A.J. Gross, A. Le Goff, M. Holzinger, Recent advances on enzymatic glucose/oxygen and hydrogen/oxygen biofuel cells: achievements and limitations, *J. Power Sources* 325 (2016) 252–263, <https://doi.org/10.1016/j.jpowsour.2016.05.133>.
- [47] W.D. Nicoll, A.F. Smith, Stability of dilute alkaline solutions of hydrogen peroxide, *Ind. Eng. Chem.* 47 (1955) 2548–2554, <https://doi.org/10.1021/ie50552a051>.
- [48] Y.V. Saltykov, G.V. Kornienko, T.A. Kenova, V.L. Kornienko, Estimation of the relative thickness of gas-diffusion electrodes of carbon-black blends in the course of electrosynthesis of the peroxide ion from, *Oxygen* 36 (2000) 4.
- [49] I. Yamanaka, T. Hashimoto, K. Otsuka, Direct synthesis of hydrogen peroxide (>1 wt%) over the cathode prepared from active carbon and vapor-grown-carbon-fiber by a new H₂–O₂ fuel cell system, *Chem. Lett.* 31 (2002) 852–853, <https://doi.org/10.1246/cl.2002.852>.
- [50] T. Murayama, I. Yamanaka, Electrosynthesis of neutral H₂O₂ solution from O₂ and water at a mixed carbon cathode using an exposed solid-polymer-electrolyte electrolysis cell, *J. Phys. Chem. C* 115 (2011) 5792–5799, <https://doi.org/10.1021/jp1109702>.
- [51] T. Murayama, S. Tazawa, S. Takenaka, I. Yamanaka, Catalytic neutral hydrogen peroxide synthesis from O₂ and H₂ by PEMFC fuel, *Catal. Today* 164 (2011) 163–168, <https://doi.org/10.1016/j.cattod.2010.10.102>.
- [52] I. Yamanaka, S. Tazawa, T. Murayama, R. Ichihashi, N. Hanaizumi, Catalytic synthesis of neutral H₂O₂ solutions from O₂ and H₂ by a fuel cell reaction, *ChemSusChem* 1 (2008) 988–992, <https://doi.org/10.1002/cssc.200800176>.
- [53] T. Kitahara, H. Nakajima, K. Mori, Hydrophilic and hydrophobic double microporous layer coated gas diffusion layer for enhancing performance of polymer electrolyte fuel cells under no-humidification at the cathode, *J. Power Sources* 199 (2012) 29–36, <https://doi.org/10.1016/j.jpowsour.2011.10.002>.
- [54] H.-H. Chen, M.-H. Chang, Effect of cathode microporous layer composition on proton exchange membrane fuel cell performance under different air inlet relative humidity, *J. Power Sources* 232 (2013) 306–309, <https://doi.org/10.1016/j.jpowsour.2013.01.079>.
- [55] S. Komini Babu, H.T. Chung, P. Zelenay, S. Litster, Resolving electrode morphology's impact on platinum group metal-free cathode performance using nano-CT of 3D hierarchical pore and ionomer distribution, *ACS Appl. Mater. Interfaces* 8 (2016) 32764–32777, <https://doi.org/10.1021/acsami.6b08844>.